

Optical properties of deposit of red blood cells suspended in dextran solutions

JOANNA STRZELECKA, MACIEJ BOSEK, BRONISŁAW GRZEGORZEWSKI*

Department of Biophysics, Collegium Medicum in Bydgoszcz, Nicolaus Copernicus University,
ul. Jagiellońska 13, 85-067 Bydgoszcz, Poland

*Corresponding author: grzego@cm.umk.pl

The optical properties of the deposit of red blood cells (RBCs) formed during sedimentation have been investigated. The human blood was obtained from healthy donors. RBCs were suspended in isotonic saline containing Dextran 70 of concentrations 2, 4 and 6 g/dl. Hematocrit of the samples was adjusted to 40%. The intensity of the light scattered by the samples of the RBC suspensions as a function of time and altitude from the bottom of a sample was measured. The region occupied by forming and sedimenting aggregates and the region occupied by deposit of the cells can be found in the sample and the temporal dependence of position of the interface separating both regions, called the deposit formation curve, can be determined. This curve exhibits the growth phase and the packing phase. We have obtained the mean intensity of light scattered by the deposit as a function of time. This intensity exhibits a monotonous decay with time over the growth as well as the packing phase, what shows that packing of the deposit occurs in the same way in both phases. The dependence from time of the mean hematocrit of the deposit was determined. We have introduced an empirical expression describing this dependence. Finally, using this dependence, we have obtained the mean intensity of light scattered by the deposit as a function of hematocrit. We have shown that this intensity follows an exponential decay. The values of an optical parameter of the deposit were found from this dependence.

Keywords: light scattering, RBC sedimentation, dextran.

1. Introduction

Red blood cell (RBC) sedimentation is a very important process from medical point of view. Linear and branched RBC aggregates called *rouleaux*, three-dimensional (3D) RBC aggregates and deposit appear during the sedimentation of a suspension of initially individual RBCs. To explain the RBC sedimentation process, it is necessary to recognize the structures that are formed by RBCs and to determine the time and altitude at which the structures appear in the sediment. Optical properties of the structures are essential in the study of light scattering by the RBC sediment. Optical properties of individual RBCs are relatively well recognized [1–3]. Although RBC aggregates were a subject of extensive studies, the knowledge about their optical properties is far from complete [4–6]. Deposit of RBCs attracted much less attention

than RBCs and aggregates [7–9]. Thus, to highlight the RBC sedimentation, the optical study of the RBC deposit is desirable.

During sedimentation, the suspension of RBCs separates into two layers: the upper layer of plasma and the lower one containing plasma and structures formed by the cells. The position of the interface between the two fractions as a function of time defines sedimentation curve. Due to the lack of theoretical understanding of the RBC sedimentation process, empirical models of the sedimentation curve are available only [10–12]. The sedimentation curves exhibit three characteristic phases. First and second phase show slow and fast fall of the position of the interface, respectively. There is no agreement as to what affects the fall of the interface during the first phase. The fast fall of the interface in the second phase reflects aggregate sedimentation. The third phase shows an asymptotic behavior of this curve. During this phase in the sediment, the packing of the cells occurs.

According to the two-region model of RBC sedimentation, there is another interface in the layer containing the cells [13]. The interface separates forming and sedimenting aggregates from the deposit of the cells. Recently, a method has been proposed to determine this interface at physiological hematocrit, where the temporal dependence of its position was called deposit formation curve [9]. This curve has the growth phase and packing phase. The deposit formation curve in the packing phase merges the sedimentation curve in its third phase. The results of the experimental studies of RBCs suspended in plasma suggest that the packing of the deposit takes place in the growth as well as in the packing phase. Furthermore, the results suggest that the packing of the deposit in the growth phase occurs in the same way as in the packing phase [9]. Up to now, the deposit attracted much less attention than the RBC aggregates. In the study of the sedimentation curve, mainly the parameters of its first and second phase were investigated [14, 15]. The data related to the deposit were presented in the study of RBC sediment formation [7–10]. Especially, the hematocrit measured at the bottom of sedimenting container characterizes the sediment of the cells [10].

RBCs aggregate in the presence of plasma or polymer solutions. In the study of the aggregation process frequently dextran solutions are utilized. Dextran solution, being a plasma substitute, induces RBC aggregation in a characteristic way. Kinetics of *rouleaux* formation has a maximum at an optimal concentration of the solution that is dependent on the molecular mass of the polymer [16, 17]. This effect of the polymer on the RBC aggregation has been extensively studied by means of light scattering, visual monitoring, ultrasound scattering, RBC sedimentation and viscometry [18–21]. Another important property of dextran is an optical clearing of blood immersed in the polymer. The optical clearing, caused by a refractive index matching, results in an increase in penetration depth of light in tissue [22, 23].

In this paper, we study the sedimentation of RBCs suspended in Dextran 70 solutions. The deposit of the cells is investigated. The goal of this paper is to estimate optical properties of the deposit of RBCs and in addition to give some insight into the process of packing of the deposit.

2. Materials and method

Human blood was obtained by venipuncture from 24 healthy donors. Blood containing anticoagulant (K_3EDTA) were centrifuged at $4\text{ }^\circ\text{C}$, at 3000 rpm for 5 min. Three times washed RBCs were suspended in isotonic saline containing Dextran 70 of concentrations 2, 4 and 6 g/dl and 0.5 g/dl human serum albumin. Hematocrit of the samples was adjusted to 40%. The samples were placed in a glass container of 20 mm height, 12 mm width and 0.5 mm depth. The experiment was performed according to the ethical guidelines laid down by the local bioethical commission.

3. Measurements apparatus

In the study, we have used experimental set-up described in [9]. The main part of the set-up is shown in Fig. 1. Light from He-Ne laser ($\lambda = 632.8\text{ nm}$) was expanded and collimated. The beam was focused by lens L_1 onto the sample S located on a motorized stage Ms . The stage moves the sample in vertical direction with velocity

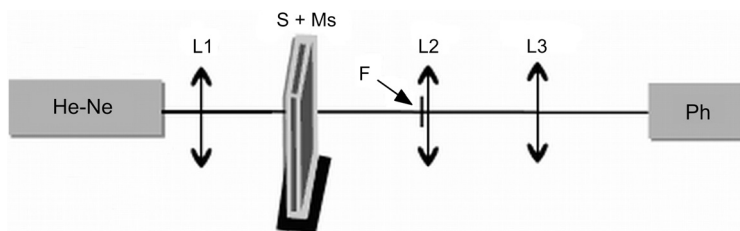


Fig. 1. Experimental set-up used to study the red blood cell sedimentation. The light-source is the He-Ne laser ($\lambda = 632.8\text{ nm}$), L_1 – L_3 are the lenses, S is the sample located on a motorized stage Ms , F is the nontransparent filter and Ph is the photomultiplier.

2 cm/min. The forward scattered light is collimated and focused by lenses L_2 and L_3 . To reduce the high intensity component of light, that appears when the beam passes through the dextran solution, the nontransparent filter F was placed in front of the lens L_2 . The scattered light was detected by a photomultiplier Ph as a function of time and altitude of the sample. Experiment was carried out at room temperature.

4. Results

Figure 2a shows the intensity of light scattered by the sample of the RBC suspension, in dextran at concentration 4 g/dl, as a function of time and altitude. The interface between the layer of highly transparent dextran solution and the fraction containing RBCs is clearly seen. Figure 2b shows the results of discrimination procedure outlined in [9] that reveals the region occupied by forming and sedimenting aggregates and the deposit of the cells. Figures 3a–3c shows the sedimentation curves $s(t)$ and deposit formation curves $d(t)$ for samples at concentrations 2, 4 and 6 g/dl of dextran.

The sedimentation curves are obtained from the discontinuity of the intensity between the region occupied by dextran solution and the fraction containing RBCs. The deposit formation curves are determined based on the procedure also described in [9].

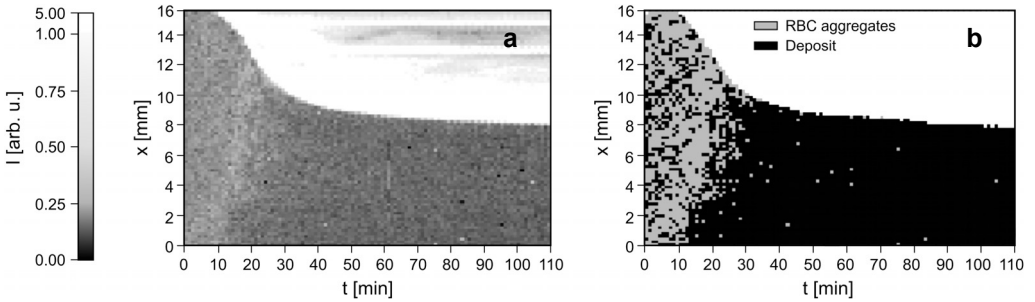


Fig. 2. The intensity of light scattered by the sample of the RBC suspension I , in dextran at concentration 4 g/dl, as a function of time t and altitude x (a); the region occupied by forming and sedimenting aggregates (gray) and the deposit of the cells (black) (b).

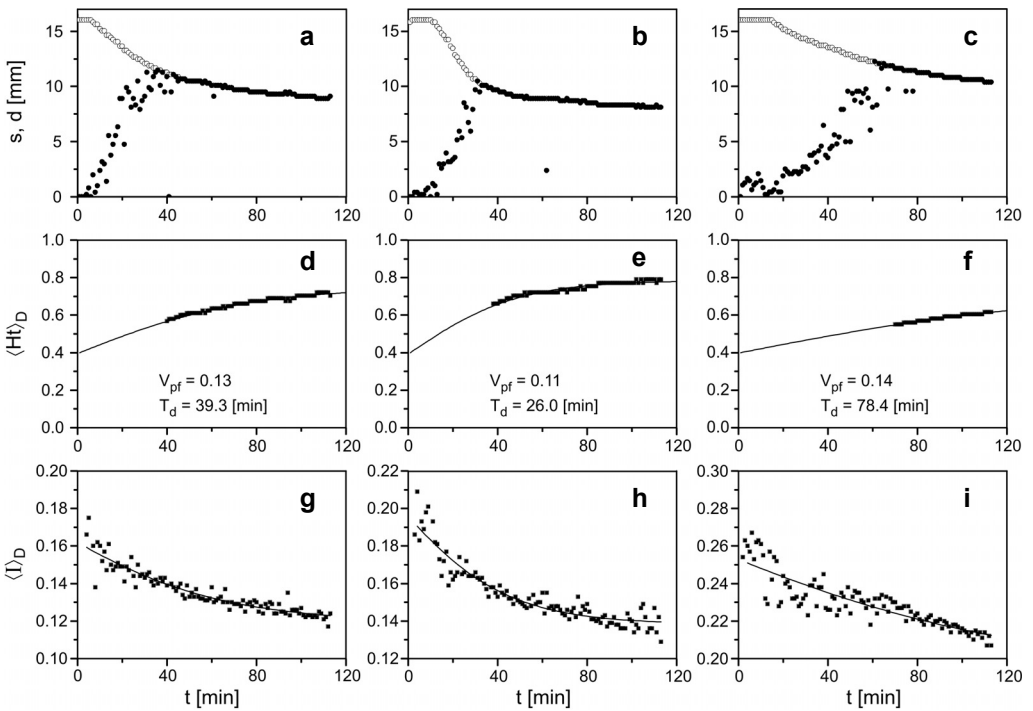


Fig. 3. The sedimentation curves $s(t)$ (open symbols) and deposit formation curves $d(t)$ (filled symbols) (a–c); the experimental mean hematocrit of the deposit (scatter plot) and its approximation, in packing phase, and extrapolation, in growth phase, calculated using expression (2) (solid line) with the characteristic time of packing T_d (d–f), and the mean intensity of light scattered by the deposit as a function of time (scatter plot) and its approximation (solid line) (g–i). The concentration of dextran of the samples is equal to 2 g/dl (a, d, g), 4 g/dl (b, e, h) and 6 g/dl (c, f, i).

The sedimentation curves exhibit three characteristic phases. The deposit formation curves exhibit two phases. First phase shows the growth of the deposit. The duration of the first phase coincides with the duration of the first and second phase of the sedimentation curve. The deposit formation curve in its second phase is identical with the sedimentation curve in its third phase.

The initial hematocrit of the sample is defined by $Ht(0) = V_e/(V_e + V_p)$, where V_e and V_p is the volume of RBCs and the solution, respectively. The hematocrit of the deposit is given by $\langle Ht \rangle_D(t) = V_{ed}(t)/V_d(t)$, where $V_{ed}(t)$ is the volume of RBCs in the deposit, $V_d(t)$ is the volume of the deposit and $\langle \dots \rangle_D$ represents an average over the deposit. Note, that in the packing phase of the deposit formation curve, all RBC aggregates settled and $V_{ed}(t) = V_e$. The data in Figs. 3d–3f shows the mean hematocrit of the deposit in the packing phase. The deposit always contains some amount of plasma. In the process of packing this amount decreases. We have assumed that packing of the deposit in the packing phase gives following dependence of its volume from time:

$$V_d(t) = (V_e + V_{pf}) + (V_p - V_{pf}) \exp\left(-\frac{t}{T_d}\right) \quad (1)$$

where V_{pf} is the volume of dextran solution in the deposit at $t \rightarrow \infty$ and T_d is the time that characterizes the packing of the deposit. Thus the mean hematocrit of the deposit takes the form

$$\langle Ht(t) \rangle_D = \frac{V_e}{(V_e + V_{pf}) + (V_p - V_{pf}) \exp\left(-\frac{t}{T_d}\right)} \quad (2)$$

The hematocrit calculated using this expression fits well the experimental data, what is shown in Figs. 3d–3f. To obtain the dependence of the hematocrit from time also in growth phase, when the RBC aggregates still sediment, we have assumed that proposed function can be used as an extrapolation of the dependence found in the packing phase (Figs. 3d–3f). In Figures 3d–3f, it is seen that the characteristic time of packing T_d obtained at dextran concentration of 4 g/dl is the smallest. The packing of the deposit for this concentration of dextran is faster than for greater as well as smaller concentrations. This slightly coincides with time of joining sedimentation and deposit formation curves for these samples (Figs. 3a–3c).

To confirm our assumptions about the validity of the approximation obtained using function (2), we have used the hematocrit values obtained by KERNICK *et al.* [10]. The measurements were performed at different time and altitude of 200 mm sample for whole blood at hematocrit 0.465. Since the deposit is formed at the bottom of the sample, we have used the hematocrit values measured at that altitude. Figure 4 shows that the formula (2) fits well the data obtained by KERNICK *et al.*

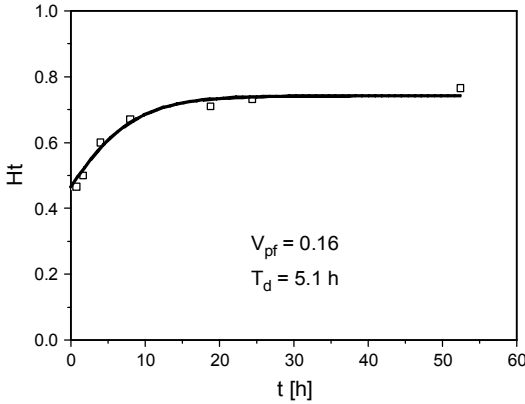


Fig. 4. The hematocrit values obtained by KERNICK *et al.* [10] measured at the bottom of the sample (scatter plot) and approximation of these data obtained using function (2) (solid line).

The experimental data shown in Fig. 2a and the deposit formation curve permit us to calculate the mean intensity of light scattered by the deposit as a function of time, which is given by the following integral:

$$\langle I \rangle_D(t) = \frac{1}{d(t)} \int_0^{d(t)} I(x, t) dx \quad (3)$$

These means as functions of time are shown in Figs. 3g–3i. Due to the irregularity of the deposit formation, the mean light intensity exhibits fluctuations.

Using the mean light intensity scattered by the deposit as well as its hematocrit as functions of time, we can obtain the mean light intensity as a function of hematocrit. These data, for the representative samples, are shown in Fig. 5. In first parts of these plots, corresponding to the growth phase of the deposit formation curve, fluctuations are clearly seen, whereas, second parts, corresponding to the packing phase, become more regular. The results shown in Fig. 5 suggest that to describe the obtained dependence, the following exponential law can be used:

$$I(\langle \text{Ht} \rangle_D) \sim \exp(-k_d \langle \text{Ht} \rangle_D d) \quad (4)$$

where k_d is an optical constant of the deposit and d is the thickness of the sample. As it is seen in Fig. 5, this expression fits well the experimental dependence. Furthermore, using that approximation and obtained dependence of hematocrit from time, we have fitted the mean light intensity as a function of time. For this dependence we also observe good agreement between received approximation and experimental data (Figs. 3g–3i).

From the fitting procedure we have determined the value of the parameter k_d for the investigated 24 samples. We have obtained group means and standard deviations

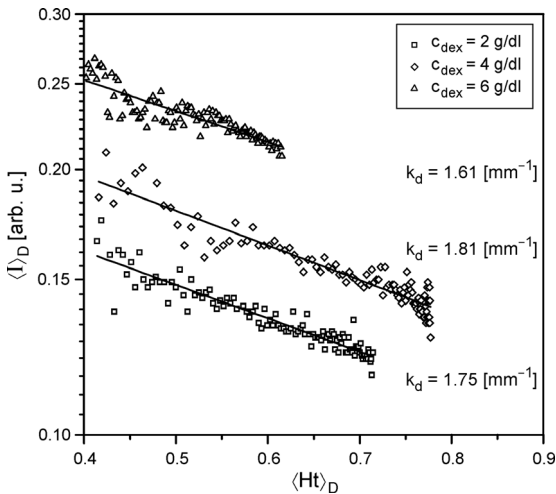


Fig. 5. The mean light intensity scattered by the deposit as a function of hematocrit, for samples at concentrations 2, 4 and 6 g/dl of dextran (scatter plots) and the exponential law approximating this dependence with the optical constant of the deposit k_d (solid lines).

for this parameter: $k_d = (1.62 \pm 0.29) \text{ mm}^{-1}$ at $c_{dex} = 2 \text{ g/dl}$, $k_d = (1.46 \pm 0.35) \text{ mm}^{-1}$ at $c_{dex} = 4 \text{ g/dl}$ and $k_d = (1.69 \pm 0.24) \text{ mm}^{-1}$ at $c_{dex} = 6 \text{ g/dl}$. Although the parameter k_d takes the lowest value at $c_{dex} = 4 \text{ g/dl}$, the means are not significantly different.

5. Discussion

In this study, the optical properties of the deposit were investigated. We have analyzed the mean intensity of light scattered by the deposit as a function of time as well as hematocrit. This analysis includes also the investigations of the temporal changes in the mean hematocrit of the deposit.

Recently, we have proposed a method that enables to determine the deposit formation curve, *i.e.*, the temporal dependence of the position of the interface between forming and sedimenting aggregates and the deposit of the cells [9]. In this study, we have determined the dependence from time of the mean hematocrit of the deposit. This dependence can be found directly in the packing phase only. We have proposed a formula that describes the hematocrit as a function of time. The changes in the hematocrit in the growth phase of the deposit formation curve were determined by an extrapolation of dependence found in the packing phase. To confirm the extrapolation procedure, we have shown that the formula fits well the data obtained by KERNICK *et al.* [10] in both phases.

The optical studies of the RBC sediment confirm that this structure changes with time and altitude [7–9]. In spite of the facts, deposit of the cells seems to be a regular structure in the sediment. The averaged intensity of light scattered by the deposit exhibits a monotonous decay with time over the growth as well as the packing phase. This dependence and the hematocrit as a function of time allow

obtaining the dependence of the averaged intensity of light scattered by the deposit from hematocrit. We have shown that this dependence follows an exponential decay with an increase in the mean hematocrit. From this dependence, an optical parameter of the deposit occurring during sedimentation of the RBCs suspended in dextran solutions has been found.

The main interest in the studies of RBCs suspended in dextran solutions is the *rouleaux* formation [16,17,19–21]. The kinetics of the RBC aggregation induced by Dextran 70 takes a maximum at concentration 3–4 g/dl [19–21]. In the investigation of *rouleaux* formation induced by Dextran 500, it was shown that this kinetics takes a maximum at concentration about 1 g/dl [19]. It is well known that dextran concentration affects optical parameters characterizing the RBC suspension. For example, Dextran 500 causes the best clearing effect in the RBC suspension at concentration of 0.5 g/dl [23]. The mean optical parameter characterizing the packing of the RBC deposit which occurred in Dextran 70, presented in this paper, exhibits minimum at concentration 4 g/dl. However, the differences are not significant.

In summary, the results of the study support the idea of two-region model of the RBC sediment formation. Our results show that packing of the deposit occurs in the same way in growth as well as in packing phase. In this way the growth of the deposit does not affect its packing. The optical properties found in this study show that the intensity of light scattered by the deposit as a function of hematocrit follows the exponential law.

Acknowledgement – This work was supported in part (J.S.) by Kuyavian–Pomeranian Voivodeship grant.

References

- [1] STEINKE J.M., SHEPHERD A.P., *Comparison of Mie theory and the light scattering of red blood cells*, Applied Optics **27**(19), 1988, pp. 4027–4033.
- [2] HAMMER M., SCHWEITZER D., MICHEL B., THAMM E., KOLB A., *Single scattering by red blood cells*, Applied Optics **37**(31), 1998, pp. 7410–7418.
- [3] FRIEBEL M., ROGGAN A., MÜLLER G., MEINKE M., *Determination of optical properties of human blood in the spectral range 250 to 1100 nm using Monte Carlo simulations with hematocrit-dependent effective scattering phase functions*, Journal of Biomedical Optics **11**(3), 2006, p. 034021.
- [4] PRIEZHEV A.V., RYABOSHAPKA O.M., FIRSOV N.N., SIRKO I.V., *Aggregation and disaggregation of erythrocytes in whole blood: Study by backscattering technique*, Journal of Biomedical Optics **4**(1), 1999, pp. 76–84.
- [5] TSINOPOULOS S.V., SELLOUNTOS E.J., POLYZOS D., *Light scattering by aggregated red blood cells*, Applied Optics **41**(7), 2002, pp. 1408–1417.
- [6] SHVARTSMAN L.D., FINE I., *Optical transmission of blood: Effect of erythrocyte aggregation*, IEEE Transactions on Biomedical Engineering **50**(8), 2003, pp. 1026–1033.
- [7] SINGH M., VATSALA T.M., *Erythrocytes sedimentation profiles under gravitational field as determined by He-Ne laser. II. Influence of erythrocyte shape*, Biorheology **19**(1–2), 1982, pp. 165–173.
- [8] SINGH M., JOSEPH K.P., *Erythrocytes sedimentation profiles under gravitational field as determined by He-Ne laser. VII. Influence of dextrans, albumin and saline on cellular aggregation and sedimentation rate*, Biorheology **24**(1), 1987, pp. 53–61.
- [9] MUTRYNOWSKA J., GRZEGORZEWSKI B., *Optical analysis of red blood cell sediment formation*, Biorheology **44**(4), 2007, pp. 285–297.

- [10] KERNICK D., JAY A.W.L., ROWLANDS S., *Erythrocyte settling*, Canadian Journal of Physiological Pharmacology **52**(6), 1974, pp. 1167–1177.
- [11] OKA S., *A physical theory of erythrocyte sedimentation*, Biorheology **22**(4), 1985, pp. 315–321.
- [12] HUNG W.T., COLLINGS A.F., LOW J., *Studies of the sedimentation of human blood*, Proceedings of the Xth International Congress on Rheology, 1988, Sydney, Australia, pp. 425–427.
- [13] REUBEN A.J., SHANNON A.G., *Some problems in the mathematical modelling of erythrocyte sedimentation*, IMA Journal of Mathematics Applied in Medicine and Biology **7**(3), 1990, pp. 145–156.
- [14] WOODLAND N.B., CORDATOS K., HUNG W.T., REUBEN A., HOLLEY L., *Erythrocyte sedimentation in columns and the significance of ESR*, Biorheology **33**(6), 1996, pp. 477–488.
- [15] HOLLEY L., WOODLAND N., HUNG W.T., CORDATOS K., REUBEN A., *Influence of fibrinogen and haematocrit on erythrocyte sedimentation kinetics*, Biorheology **36**(4), 1999, pp. 287–297.
- [16] NEU B., MEISELMAN H.J., *Depletion-mediated red blood cell aggregation in polymer solutions*, Biophysical Journal **83**(5), 2002, pp. 2482–2490.
- [17] NEU B., WENBY R., MEISELMAN H.J., *Effects of dextran molecular weight on red blood cell aggregation*, Biophysical Journal **95**(6), 2008, pp. 3059–3065.
- [18] PRIBUSH A., MEYERSTEIN N., *Methodological aspects of erythrocyte aggregation*, Recent Patents on Anti-Cancer Drug Discovery **2**(3), 2007, pp. 240–245.
- [19] NASH G.B., WENBY R.B., SOWEMIMO-COKER S.O., MEISELMAN H.J., *Influence of cellular properties on red cell aggregation*, Clinical Hemorheology **7**, 1987, pp. 93–108.
- [20] BOYNARD M., LELIERE J.C., *Size determination of red blood cell aggregates induced by dextran using ultrasound backscattering phenomenon*, Biorheology **27**(1), 1990, pp. 39–46.
- [21] BARSHTEIN G., TAMIR I., YEDGAR S., *Red blood cell rouleaux formation in dextran solution: dependence on polymer conformation*, European Biophysics Letter **27**(2), 1998, pp. 177–181.
- [22] TUCHIN V.V., XU X.Q., WANG R.K., *Dynamic optical coherence tomography in studies of optical clearing, sedimentation, and aggregation of immersed blood*, Applied Optics **41**(1), 2002, pp. 258–271.
- [23] XU X., WANG R.K., ELDER J.B., TUCHIN V.V., *Effect of dextran-induced changes in refractive index and aggregation on optical properties of whole blood*, Physics in Medicine and Biology **48**(9), 2003, pp. 1205–1221.

Received April 10, 2009